

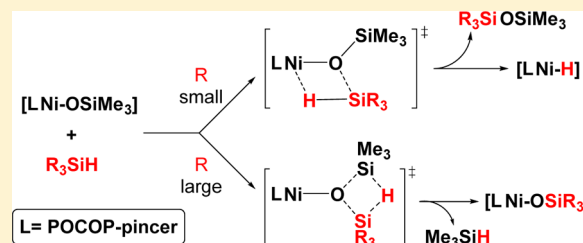
Reactions of Phenylhydrosilanes with Pincer–Nickel Complexes: Evidence for New Si–O and Si–C Bond Formation Pathways

Jingjun Hao, Boris Vabre, and Davit Zargarian*

Département de Chimie, Université de Montréal, Montréal, Québec H3C 3J7, Canada

S Supporting Information

ABSTRACT: This contribution presents evidence for new pathways manifested in the reactions of the phenylhydrosilanes $\text{Ph}_n\text{SiH}_{4-n}$ with the pincer complexes $(\text{POC}_{\text{sp}^3\text{OP}}\text{Ni}(\text{OSiMe}_3)_3)$, **1-OSiMe₃**, and $(\text{POC}_{\text{sp}^3\text{OP}}\text{Ni}(\text{OSiMe}_3)_2)$, **2-OSiMe₃** ($\text{POC}_{\text{sp}^3\text{OP}} = 2,6-(i\text{-Pr}_2\text{PO})_2\text{C}_6\text{H}_3$; $\text{POC}_{\text{sp}^3\text{OP}} = (i\text{-Pr}_2\text{POCH}_2)_2\text{CH}$). Excess PhSiH_3 or Ph_2SiH_2 reacted with **1-OSiMe₃** to eliminate the disilyl ethers $\text{Ph}_n\text{H}_{3-n}\text{SiOSiMe}_3$ ($n = 1$ or 2) and generate the nickel hydride species **1-H**. Subsequent reaction of the latter with more substrate formed corresponding nickel silyl species **1-SiPhH₂** or **1-SiPh₂H** and generated multiple Si-containing products, including disilanes and redistribution products. The reaction of **1-OSiMe₃** with excess $\text{Ph}_2\text{SiH}_2/\text{Ph}_2\text{SiD}_2$ revealed a net KIE of ca. 1.3–1.4 at room temperature. Treating **1-OSiMe₃** with excess Ph_3SiH also gave **1-H** and the corresponding disilyl ether $\text{Ph}_3\text{SiOSiMe}_3$, but this reaction also generated the new siloxide **1-OSiPh₃** apparently via an unconventional σ -bond metathesis pathway in which the Ni center is not involved directly. The reaction of excess PhSiH_3 and **2-OSiMe₃** gave polysilanes of varying solubilities and molecular weights; NMR investigations showed that these polymers arise from Ni(0) species generated in situ from the reductive elimination of the highly reactive hydride intermediate, **2-H**. The stoichiometric reactions of **2-OSiMe₃** with Ph_2SiH_2 and Ph_3SiH gave, respectively, siloxides **2-OSiPh₂(OSiMe₃)** and **2-OSiPh₃**. Together, these results demonstrate the strong influence of pincer backbone and hydrosilane sterics on the different reactivities of **1-OSiMe₃** and **2-OSiMe₃** toward $\text{Ph}_n\text{SiH}_{4-n}$ (dimerization, polymerization, and redistribution vs formation of new siloxides). The mechanisms of the reactions that lead to the observed Si–O, Si–C, and Si–Si bond formations are discussed in terms of classical and unconventional σ -bond metathesis pathways.



INTRODUCTION

A number of transition metal complexes are known to be viable catalysts for the dehydrogenative polymerization of hydrosilanes to polysilanes.^{1,2} To date, the most efficient catalysts are Ti- and Zr-based metallocenes, whereas systems based on late metals are generally less efficient and suffer from side reactions such as redistribution (scrambling of Si substituents).³ Mechanistic studies have concluded that systems based on d^0 metals break substrate Si–H bonds and form new Si–Si linkages through successive, concerted constant-oxidation-state σ -bond metathesis steps (Scheme 1, path A).⁴ In contrast, the oligo- and polymerization of hydrosilanes by low-valence late transition metals can, in principle, involve conventional Si–H oxidative addition and Si–Si reductive elimination steps (Scheme 1, path B).⁵

In the case of Ni-catalyzed polymerization of hydrosilanes, mechanisms proceeding via oxidative addition/reductive elimination steps would seem more realistic for zero-valent precursors and intermediates,⁶ but some Ni^{II} species have been suspected of reacting with PhSiH_3 via σ -bond-metathesis-type transition states.⁷ In the absence of sufficient data on this topic, it is not known which factors contribute to the preference of one pathway over the other. Another obscure question in this context pertains to the factors that favor one or the other of the two competing reactivities, Si–Si bond making steps that

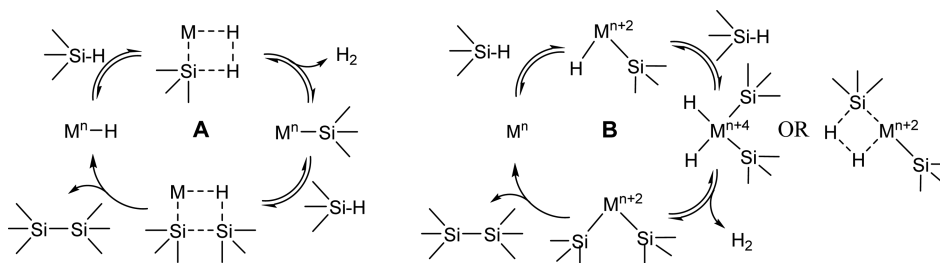
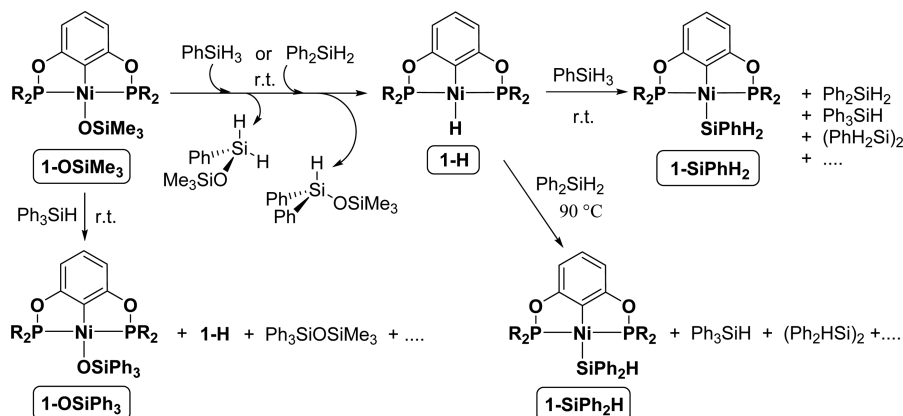
contribute productively to the polymerization process versus the Si–R bond making/breaking steps that lead to undesired redistribution reactions ($R = \text{alkyl}$ or aryl substituents). The latter side reactions are quite prevalent in Ni-based systems and often indicate the involvement of multiple active intermediates in the catalytic manifold. That some of these intermediates are paramagnetic species further complicates mechanistic studies.

We have been interested in probing the reactivities of hydrosilanes with Ni complexes of different ligands,⁸ and it occurred to us that some of the above-mentioned mechanistic questions might be more effectively examined by conducting our reactivity studies using thermally stable, diamagnetic Ni^{II} complexes. Given the aptitude of tridentate pincer ligands to securely anchor a divalent Ni center and generate highly stable complexes,⁹ we have undertaken to study the reactivities of hydrosilanes with Ni^{II} precursors based on two different POCOP-type pincer ligands, namely, $2,6-(i\text{-Pr}_2\text{PO})_2\text{C}_6\text{H}_3$ ($\text{POC}_{\text{sp}^3\text{OP}}$) and $(i\text{-Pr}_2\text{POCH}_2)_2\text{CH}$ ($\text{POC}_{\text{sp}^3\text{OP}}$).¹⁰ The original objective of this study was to establish whether or not the pincer ligand backbone can influence the reactivity of its complexes for dehydrogenative oligo- or polymerization versus redistribution reactions. We began by examining the reactivities

Received: September 29, 2015

Published: November 12, 2015

Scheme 1. Proposed Mechanisms for Dehydrogenative Oligo- and Polymerization of Hydrosilanes

Scheme 2. Different Reactivities of 1-OSiMe₃ with Ph_nSiH_{4-n}

of Ph_nSiH_{4-n} with (POC_{sp}²OP)Ni(OSiMe₃), **1-OSiMe₃**, and (POC_{sp}³OP)Ni(OSiMe₃), **2-OSiMe₃**.¹¹ Our rationale for using these precursors was twofold: the relatively reactive Ni-OSiMe₃ moiety should facilitate the Si-H bond activation process, and the ultimate fate of the readily trackable OSiMe₃ fragment might provide valuable mechanistic clues. This strategy has been validated by the finding that the presence of Ni-O-Si linkages in the precursors facilitates both the initial Si-H activation step and the subsequent detection of side products formed in various stoichiometric and catalytic reactions. The results presented herein also help rationalize the unanticipated formation of the siloxide derivatives **1-OSiPh₃** and **2-OSiPh₃** (from Ph₃SiH and **1-** or **2-OSiMe₃**) and **2-OSiPh₂OSiMe₃** (from Ph₂SiH₂ and **2-OSiMe₃**) and provide a mechanistic framework for understanding how these systems might promote hydrosilane redistribution. The relationship between hydrosilane redistribution and dehydrocoupling promoted by analogous POC_{sp}²OP-Ir systems has also been examined recently by Waterman's group;¹² their findings of the importance of pincer ligand and silane substituent sterics echo some of our observations and will be discussed herein.

RESULTS AND DISCUSSION

The reactions of the siloxide precursors **1-OSiMe₃** and **2-OSiMe₃** with phenylsilanes were conducted in J. Young NMR tubes to facilitate real-time monitoring of kinetic profiles and detection of products and intermediates. Synthesis-scale reactions were also carried out to allow isolation of various products. The results of these experiments are described in the following sections.

Reactivities of Ph_nSiH_{4-n} with 1-OSiMe₃. Treating **1-OSiMe₃** with excess PhSiH₃ or Ph₂SiH₂ gave, initially, Guan's hydride **1-H**¹³ and the corresponding disilyl ethers PhH₂SiOSiMe₃ or Ph₂SiHOSiMe₃ (Scheme 2). The latter

were identified by GC/MS analyses of the reaction mixtures (PhH₂SiOSiMe₃: *M_w* = 196, Ph₂SiHOSiMe₃: *M_w* - Me = 257; Figures S1 and S2), whereas **1-H** was identified on the basis of its characteristic NMR signals (³¹P δ: 207.8; ¹H δ: -7.9, *t*, ²*J*_{H-P} = 55 Hz).

The in situ generated hydride continued to react further, albeit more sluggishly, with excess substrate (PhSiH₃ or Ph₂SiH₂), giving multiple species (Scheme 2).¹⁴ For instance, the reaction with 10 equiv of PhSiH₃ slowly converted **1-H** to the corresponding silyl complex **1-SiPhH₂** (ca. 90% conversion after 1 week at room temperature) and generated Ph₂SiH₂, (PhH₂Si)₂^{4a,7a,12,15} and trace amounts of Ph₃SiH as well as other unidentified species (Figure S3-S6). The reaction of in situ generated **1-H** with excess Ph₂SiH₂ was even slower, requiring heating at 90 °C over 1 week to generate **1-SiPh₂H**, Ph₃SiH, (Ph₂HSi)₂, and trace amounts of other unidentified species (Figure S7-S9).

The reaction of **1-OSiMe₃** with Ph₃SiH also gave **1-H** and the corresponding disilyl ether Ph₃SiOSiMe₃ (*M_w* = 348; Figure S10), but instead of a new silyl derivative, we obtained in this case the siloxide derivative **1-OSiPh₃** (Scheme 2). The latter is a known compound that has been prepared from the metathetic reaction of **1-Cl** with KOSiPh₃ and fully characterized,^{11c} whereas the silyl derivatives **1-SiPhH₂** and **1-SiPh₂H** are new compounds. The isolation and complete characterization of these silyl derivatives and a discussion of the various pathways leading to the products observed in these three reactions will be presented later.

Reactivities of Ph_nSiH_{4-n} with 2-OSiMe₃. Compared to the above-described reactions of complex **1-OSiMe₃**, we observed very different reactivities with the closely related siloxide **2-OSiMe₃**, including the formation of polysilanes with PhSiH₃ and Ph₂SiH₂. For example, addition of 200 equiv of PhSiH₃ to a 0.025 M benzene solution of **2-OSiMe₃** at room

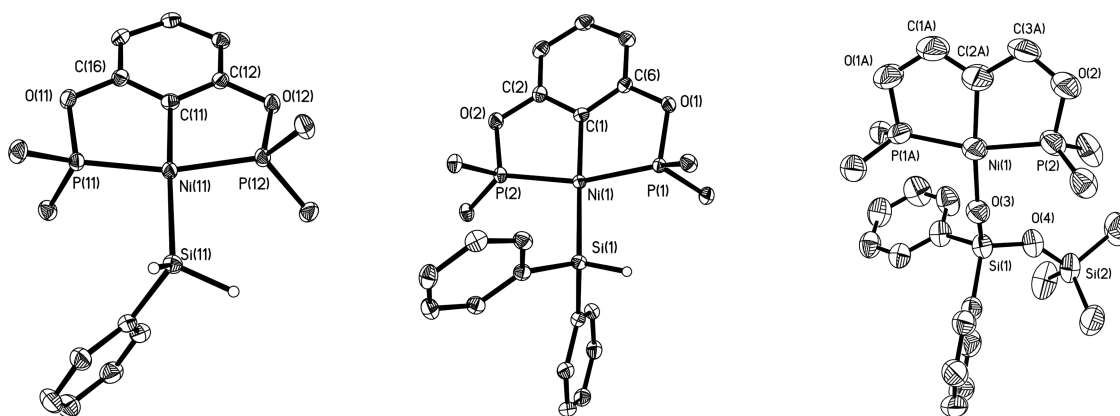
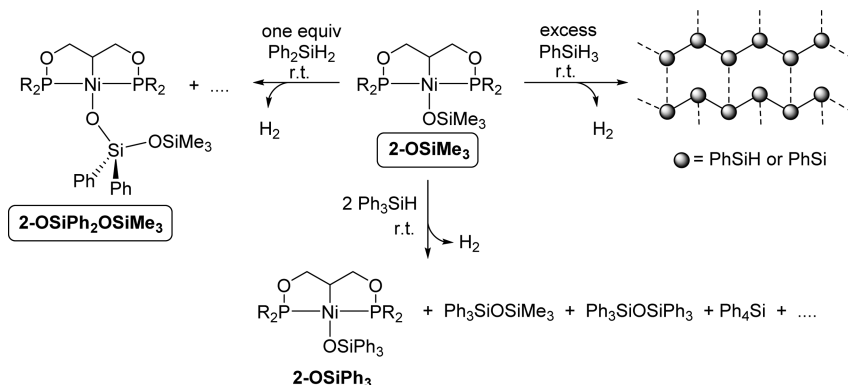
Scheme 3. Reactivities of 2-OSiMe₃ with PhSiH₃, Ph₂SiH₂, and Ph₃SiH

Figure 1. Solid structures of 1-SiPhH₂, 1-SiPh₂H, and 2-OSiPh₂OSiMe at the 50% probability level. All hydrogen atoms except those on silicon atoms and methyl groups on the *i*-Pr group are omitted for clarity.

temperature led to an immediate and vigorous effervescence and a gradual darkening of the reaction mixture. The effervescence subsided somewhat after ca. 5 min, but did not stop completely until about 15 h when a solid had precipitated. Addition of THF to the final mixture followed by further stirring over 3 h, evaporation, and washing with hexane and acetonitrile gave a white solid that corresponded to ca. 60% yield (on the basis of initial monomer mass). Analysis of this sparingly soluble product by ¹H NMR (C₆D₆, Figure S11) showed broad resonances for Si–C₆H₅ (6.5–8.0 ppm) and Si–H (5.0–5.7 ppm) in ca. 10:1 intensity ratio, and GPC analysis (Figure S12) showed multiple components, one of which displayed *M_n* and *M_w* values of 3900 and 23 246 g/mol, respectively.

Interestingly, the final products of the reactions of 2-OSiMe₃ with PhSiH₃ varied considerably depending on reaction conditions and especially workup procedures. For instance, a solid sample obtained from a reaction run in toluene and worked-up by simple evaporation showed a Si–Ph/Si–H intensity ratio of 5:1 (Figure S13) and GPC parameters typical of short-chain, linear (PhSiH)_{*n*} oligomers: *M_n* = 1361 g/mol and *M_w* = 1399 g/mol (Figure S14). In contrast, conducting the polymerization in neat PhSiH₃ led to a more vigorous evolution of gas and produced a nearly insoluble solid precipitate that defied analysis by GPC or NMR. These observations suggest that 2-OSiMe₃ can convert PhSiH₃ into fairly monodispersed linear oligo(phenylsilane) or polydispersed polymers featuring fairly high numbers of Si–Si linkages and possessing varying degrees of cross-linking depending on the reaction conditions (Scheme 3).

The analogous reaction of 2-OSiMe₃ with excess Ph₂SiH₂ (room temperature, toluene) generated a small amount of gas, and over time, small particles of a red solid formed on the sides of the reaction flask. We suspected that this material was a polymer derived from Ph₂SiH₂ but could not confirm this hypothesis. Treating 2-OSiMe₃ with only 1 equiv of Ph₂SiH₂ gave traces of the aforementioned red solid in addition to a yellow solid that was isolated in ca. 35% yield and identified (vide infra) as the new siloxide derivative 2-OSiPh₂OSiMe₃ (Scheme 3). This compound did react with Ph₂SiH₂ but did so very slowly, implying that it was not involved in the vigorous reaction leading to formation of the red solid.

Finally, the reaction of 2-OSiMe₃ with excess Ph₃SiH resulted in a very complex mixture of products (Scheme 3). That 2-OSiMe₃ competes with an in situ generated derivative 2-X for reaction with Ph₃SiH was evident from incomplete conversions with stoichiometric amounts of substrate. For instance, the room temperature reaction of 2-OSiMe₃ with 1 equiv of Ph₃SiH gave only ca. 50% conversion, even after 10 days of stirring (Figure S15). Addition of an additional 1 equiv of Ph₃SiH to this mixture led to ca. 93% conversion of 2-OSiMe₃ (Figure S16) and gave hydrogen gas (detected by ¹H NMR), Ph₄Si (Figure S17) and Ph₃SiOSiMe₃ (identified by GC/MS, Figure S18), and two solids identified by X-ray diffraction studies as the known compounds 2-OSiPh₃^{11c} and Ph₃SiOSiPh₃.¹⁶

Isolation and Characterization of 1-SiPhH₂, 1-SiPh₂H, and 2-OSiPh₂OSiMe₃. The silyl derivatives were isolated from the reactions of 1-OSiMe₃ with PhSiH₃ or Ph₂SiH₂ in 21–25% yields. These poor yields reflect the complicated workup

Table 1. Bonding Parameters of Complexes 1-SiPh₂H₂, 1-SiPh₂H, and 2-OSiPh₂OSiMe₃

	1-SiPh ₂ H ₂	1-SiPh ₂ H	2-OSiPh ₂ OSiMe ₃
Ni–C	1.9124(12)	1.9188(13)	1.941(19), 1.986(16)
Ni–Si/Ni–O	2.2826(4)	2.3040(4)	1.874(2)
Ni–P1	2.1206(4)	2.1314(4)	2.1450(11)
Ni–P2	2.1322(4)	2.1494(4)	2.150(7), 2.198(7)
O–Si			1.569(3)
P–Ni–P	164.542(16)	163.528(17)	164.5(2), 165.5(2)
C–Ni–Si/C–Ni–O	176.61(4)	174.26(4)	170.4(6), 167.8(6)
P1–Ni–X	95.180(15)	95.354(15)	95.10(8)
P2–Ni–X	100.277(15)	100.466(15)	98.8(2), 98.5(2)
Ni–O–Si			153.53(16)

procedures required for treating reaction mixtures that contain multiple side products. Indeed, in addition to the products shown in Scheme 2, the reactions of 1-H with PhSiH₃ and Ph₂SiH₂ also generate small amounts of complexes that we believe to be various silyl species 1-SiR₃; this assignment is based on the closeness of their ³¹P NMR signals to those of the isolated and fully characterized species 1-SiPhH₂ and 1-SiPh₂H (ca. 200 ppm, vide infra). The new siloxide 2-OSiPh₂OSiMe₃ was isolated in 34% yield from the stoichiometric reaction of 2-OSiMe₃ with Ph₂SiH₂ (added dropwise at room temperature).

The NMR spectra of these three diamagnetic complexes showed features that are similar to those of previously studied analogues and were consistent with the proposed structures (Figures S19–S27). For instance, the ³¹P NMR spectra showed resonances upfield of corresponding resonance for the Ni–H species, i.e., 199.7 ppm for 1-SiPhH₂ and 200.7 ppm for 1-SiPh₂H, whereas the ¹H NMR spectra showed the anticipated triplets for the Si–H moieties in NiSiPhH₂ (4.74 ppm, ³J_{P–H} = 7.5 Hz) and Ni–SiPh₂H (5.43 ppm, ³J_{P–H} = 12.5 Hz)¹⁷ in addition to virtual triplets for P–C–CH₃ nuclei. The characteristic ν(Si–H) absorptions were detected in the IR spectra, appearing at 2028 cm⁻¹ (s) in 1-SiPhH₂ and 2126 cm⁻¹ (s) in 1-SiPh₂H. The ³¹P NMR resonance of 2-OSiPh₂OSiMe₃ at ca. 177 ppm was in the region characteristic of 2-OSiR₃,^{11c} whereas its ¹H and ¹³C NMR signals were comparable to the corresponding signals in previously reported siloxide complexes.¹⁸ For instance, the ¹H and ¹³C NMR signals for the OSi(CH₃)₃ moiety in 2-OSiPh₂OSiMe₃ appear at 0.12 and 2.4 ppm, respectively, versus 0.24 and 5.5 for the corresponding signals in 2-OSiMe₃.^{11c}

The solid-state structures of these complexes confirmed the above assignments (Figure 1). The Ni center in both silyl compounds adopts a lightly distorted square planar geometry, and most structural parameters (Table 1) are normal for this family of complexes,^{11,19} including smaller than ideal trans P–Ni–P angles of ca. 163–165°. The Si–H hydrogen atoms were located in the electron density map and refined isotropically at 1.40–1.42 Å. The large separation between the nickel center and the Si–H hydrogen atoms (>3.1 Å) and the large Ni–Si–H angles in both 1-SiPhH₂ and 1-SiPh₂H (>110°) indicate the absence of agostic Ni–H interactions.²⁰ The Ni–Si distances (ca. 2.28 Å in 1-SiPhH₂ and ca. 2.30 Å in 1-SiPh₂H) are in the expected range for Ni–silyl species (2.21–2.37 Å),^{17,21} whereas the somewhat longer Ni–C distances in these complexes relative to the corresponding distances in the bromo and OSiMe₃ derivatives (ca. 1.91–1.92 Å vs ca. 1.88–1.89 Å) are consistent with the greater trans influence of the silyl moiety.

The solid-state structure of 2-OSiPh₂OSiMe₃ confirmed the spectral assignments and showed that the Ni center adopts a

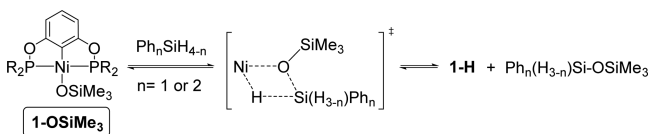
lightly distorted square planar geometry. The Ni–O bond distance (1.874(2) Å, Table 1) is in the normal range for Ni–OR complexes.²² Similarly, the Si1–O3 distance (1.569(3) Å) is comparable to the corresponding distances found in complexes featuring a M–OSiMe₃ moiety,^{18c,23} but it is significantly shorter than Si1–O4 (1.654(2) Å) and Si2–O4 (1.631(3) Å) distances. The latter are, however, comparable to Si–O bond distances found in organic siloxy structures.²⁴ The Ni–O–Si angle of 154° implies some degree of O → Si electron delocalization that serves presumably to minimize the d_π–p_π destabilizing interactions anticipated in square planar d⁸ systems featuring M–heteroatom linkages.²⁵

Probing Kinetic Isotope Effects in the Reaction of 1-OSiMe₃ with Ph₂SiH₂. As mentioned at the outset of this report, a central question in the context of metal-promoted dehydrogenative transformations of hydrosilanes is whether the crucial Si–H bond activation and Si–Si bond formation steps proceed through classical oxidative addition/reductive elimination sequences or constant-oxidation-state σ-bond metathesis steps. Tilley's group has used a number of experimental and theoretical indices, including kinetic isotope effect (KIE) measurements, to establish that the latter scenario is operative in the reactions of group 3 and group 4 metallocenes.²⁶ For instance, a k_H/k_D value of 2.5–2.7 was found for the 343 K reaction of CpCp*Hf(SiR₃)Cl with PhSiH₃/PhSiD₃,^{4a,27} whereas the 193–243 K reaction of Cp*₂ScMe with Ph₂SiH₂/Ph₂SiD₂ showed a k_H/k_D value of 1.15.²⁸ Both of these reactions are thought to proceed by σ-bond metathesis, and the relatively small k_H/k_D value for the Sc system is thought to result from an early transition state wherein the Si–H/D bond is mostly intact. There have been fewer KIE measurements for reactions of late transition metal complexes with hydrosilanes, but our group has reported a k_H/k_D value of ca. 9.8 for the 313 K reaction of PhSiH₃/PhSiD₃ with (1-Me-indenyl)Ni(PMe₃)₂, an efficient initiator for dehydrogenative oligomerization of PhSiH₃.^{7a}

In search of a mechanistic clue for the reactivities of our complexes, we have probed the initial reaction of 1-OSiMe₃. Ph₂SiH₂ was selected for this study because its much slower reaction with the initial product of the reaction, 1-H, would facilitate measurements of product ratios. The reaction with Ph₂SiD₂ generated the anticipated deuteride 1-D, which was identified on the basis of the characteristic 1:1:1 triplet ³¹P resonance (²J_{P–D} ≈ 8 Hz, Figure S28); a competition study was then conducted with 1-OSiMe₃ and excess Ph₂SiH₂/Ph₂SiD₂, revealing a net KIE of ca. 1.3–1.4 at room temperature (Figures S29 and S30).²⁹ This value is similar to the corresponding KIE values of 1.15 reported by Tilley for Ph₂SiH₂/Ph₂SiD₂ (vide supra) and also the value of 1.62 reported by Hartwig for the

exchange of methyl in CpRu(PPh₃)₂Me with the hydrogen in catecholborane;³⁰ both of these reactions are believed to proceed through a concerted, four-centered transition state. The closeness of these KIE values to that for the reaction of **1-OSiMe₃** with Ph₂SiH₂ suggests that the Ni-promoted reactions under discussion here likely proceed through constant-oxidation-state, four-centered transition states characteristic of σ -bond metathesis mechanisms, as illustrated in **Scheme 4**.

Scheme 4. Proposed Pathway for the Initial Reactions of 1-OSiMe₃ with Ph_nSiH_{4-n} and Ph₂SiH₂



Nevertheless, we acknowledge that the observed KIE value can equally reasonably imply an oxidative addition mechanism; thus, an alternative mechanism based on stepwise pathways involving Ni^{IV} intermediates cannot be ruled out.³¹

The transition state shown in **Scheme 4** is logical because it places the larger group at the less-hindered β position of the transition state. This scenario is also consistent with the above-discussed findings, including the fact that the initial reaction of the Ni-OSiMe₃ moiety with Ph_nSiH_{4-n} gives a hydride species and disilyl ethers and not the silanol Me₃SiOH or polysiloxanes arising from its decomposition.

Mechanistic Insights Pertaining to the Reaction of 1-OSiMe₃ with Ph₃SiH. The observed formation of **1-H** and Ph₃SiOSiMe₃ from this reaction can be accounted for by invoking a constant-oxidation-state transition state similar to that proposed above for the analogous reaction with Ph₂SiH₂ (**Scheme 4**). Recall, however, that the Ph₃SiH reaction also generates **1-OSiPh₃**, which is a product that cannot arise directly from **1-OSiMe₃** via the same type of σ -bond metathesis reaction; this product is also unable to form via a classical oxidative addition/reductive elimination sequence. To gain insight on the reaction of **1-OSiPh₃** with Ph₃SiH, we have closely monitored a few reactions that produce or consume **1-OSiPh₃** with the following results.

Scheme 5 outlines different pathways leading to **1-OSiPh₃**, including a two-step route that initially gives **1-H** and the disilyl ether Ph₃SiOSiMe₃ (path A), followed by their subsequent reaction to give **1-OSiPh₃** (path B). Tests with independently prepared reactants showed that **1-H**¹³ and Ph₃SiOSiMe₃ (prepared from Ph₃SiOK and ClSiMe₃) do react to give **1-**

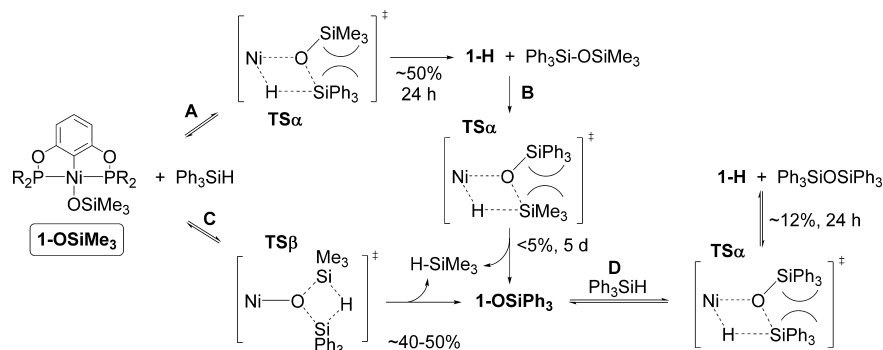
OSiPh₃ (**Figures S31 and S32**),³² but the very sluggish rate of this reaction (2–3% conversion over 5 days) implies that another route must be responsible for the formation of **1-OSiPh₃** in the reaction of **1-OSiMe₃** with Ph₃SiH. We also considered the opposite scenario, i.e., that **1-OSiPh₃** forms initially and reacts subsequently with Ph₃SiH to give **1-H** (path D), but this, too, was dismissed on the basis of the following observations: the reaction of Ph₃SiH with **1-OSiPh₃** gave ca. 12% conversion to **1-H** over 24 h even under sonication (**Figures S33 and S34**), whereas the analogous reaction with **1-OSiMe₃** gave more than 50% conversion under the same conditions.

An interesting clue to the above puzzle was presented by the observation that the relative amounts of **1-H** and **1-OSiPh₃** generated in the reactions of **1-OSiMe₃** and Ph₃SiH depend on the amount of Ph₃SiH used, with **1-OSiPh₃** being the major product with substoichiometric amounts of Ph₃SiH, whereas excess Ph₃SiH led to the formation of greater proportions of **1-H** (**Figures S35–S37**). Putting this finding together with the above observations, we conclude that **1-OSiPh₃** is generated independently of **1-H** via a distinct pathway (path C) whereas **1-H** results via two different pathways involving the reactions of Ph₃SiH + **1-OSiMe₃** (paths A and B) and Ph₃SiH + **1-OSiPh₃** (path D). As shown in **Scheme 5**, the paths leading to **1-H** likely proceed through the “conventional” transition states TS α that exchange the Ni–O and H–Si bonds, whereas **1-OSiPh₃** can form through the “unconventional” metathesis-like transition state TS β exchanging the O–Si bond in **1-OSiMe₃** and the Si–H bond in Ph₃SiH.

We recognize that the TS β proposed above might appear controversial by virtue of not involving a transition metal center whose d orbitals are normally considered to be required for such otherwise Woodward–Hoffmann disallowed rearrangements.³³ However, it is instructive to recall that 2s+2s type suprafacial–suprafacial [1,2] shifts are only symmetry-forbidden in carbon chemistry. Indeed, when they involve migrating groups such as Si-based fragments that can adopt pentacoordination at the transition state, such reactions should have much lower activation barriers. This phenomenon also underlies the energetic accessibility of the dyotropic [1,2]-SiR₃ shifts such as Brook/retro Brook rearrangements commonly seen in organosilanes.³⁴ Thus, we believe that the pathways proceeding through both the above-described transition states TS α and TS β are realistic.

Consideration of these transition states allows us to interpret the observed reactivities of **1-OSiMe₃** with Ph_nSiH_{4-n} as follows. The initial reactions with PhSiH₃ and Ph₂SiH₂ go

Scheme 5. Proposed Pathways for Reactions of 1-OSiMe₃ with Ph_nSiH_{4-n}



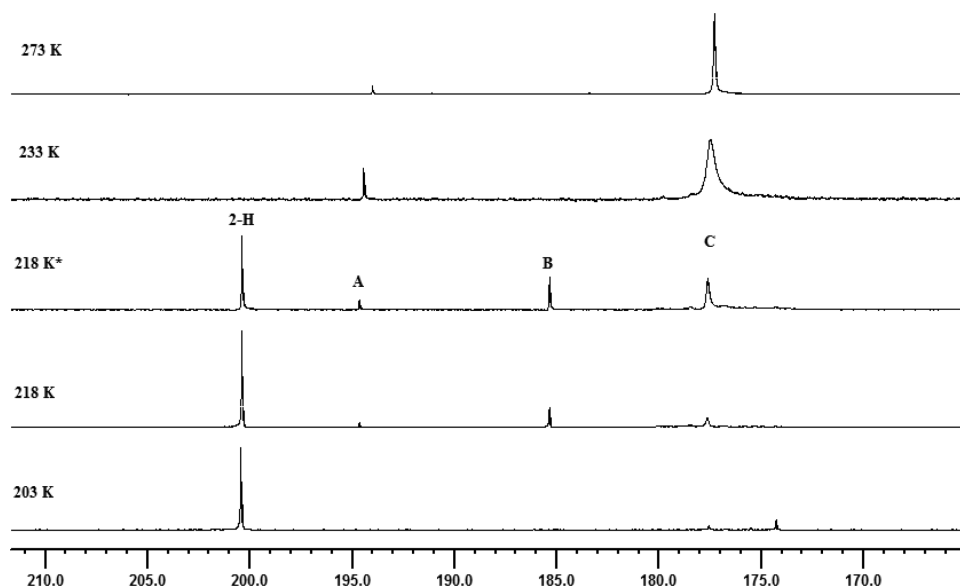
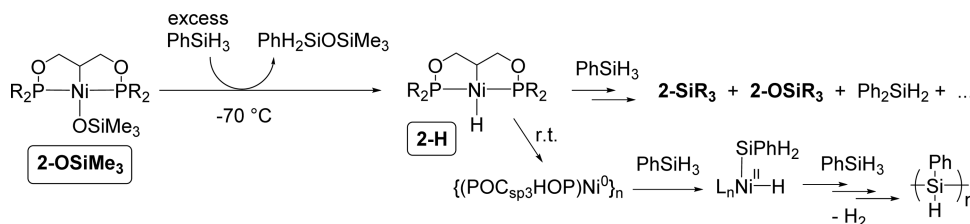


Figure 2. ^{31}P NMR monitoring of the reaction between **2-OSiMe₃** with 8 equiv of PhSiH₃ (203–273 K in C_7D_8). The spectrum was recorded after keeping the sample at 218 K for 10 min.

Scheme 6. Variable Temperature Reactions of PhSiH₃ with **2-OSiMe₃**



through the more conventional $\text{TS}\alpha$ shown in [Scheme 4](#), whereas the reaction with Ph_3SiH goes through both $\text{TS}\alpha$ and a less common pathway $\text{TS}\beta$ involving the OSiMe_3 moiety but not the Ni center ([Scheme 5](#)). The different reactivity with Ph_3SiH is presumably due to the greater steric repulsion between the Ph_3Si and SiMe_3 moieties ([Scheme 5](#)).^{35,35,36} Significantly, both of these pathways result in the formation of a new Si–O bond in preference over Ni–Si or Si–Si bonds.

Mechanistic Insights Pertaining to the Reaction of **2-OSiMe₃ with PhSiH_3 .** Recall that the reactions of **2-OSiMe₃** with PhSiH_3 and Ph_2SiH_2 lead primarily to Si–Si bond formation, whereas silane redistribution appears to be the main outcome of the reaction with Ph_3SiH . Significantly, no silyl or hydride derivative was detected in any of these reactions even at room temperature, but formation of hydride derivative **2-H** was inferred from the detection of the disilyl ethers $\text{Ph}_2\text{HSiOSiMe}_3$ and $\text{Ph}_3\text{SiOSiMe}_3$. In an effort to better understand these reactivities, we have examined the reactions of **2-OSiMe₃** with PhSiH_3 closely, including at low temperatures, with the following results.

Low-temperature NMR analysis of a toluene- d_8 solution of **2-OSiMe₃** with ca. eightfold excess of PhSiH_3 showed the formation of a new hydride species represented by a triplet at -9.06 ppm in the ^1H NMR spectrum ($^2J_{\text{P-H}} = 57$ Hz; [Figures S38](#)) and a singlet resonance at 200.4 ppm in the $^{31}\text{P}\{^1\text{H}\}$ NMR spectrum ([Figure 2](#), 203 K). This new species (**2-H**) likely arises through the expulsion of $\text{Me}_3\text{SiOSiPhH}_2$ ([Scheme 6](#)).

Warming the sample brought about a gradual decline in the intensity of the new ^{31}P signal, and over time, it was replaced by two new transient peaks at ca. 195 ppm (A) and ca. 185 ppm (B) plus a third peak at ca. 177 ppm (C). The latter turned out to be the final P-containing product ([Figure 2](#)). The chemical shift of the transient signal A is in a region characteristic of Ni–SiR₃ species,³⁷ whereas signal C is in the Ni–OSiR₃ chemical shift range (175–180 ppm). The identity of the species giving rise to signal B has not yet been established.³⁸ The room-temperature ^1H NMR spectrum of this sample ([Figures S39 and S40](#)) showed unreacted PhSiH_3 , H_2 , a small amount of Ph_2SiH_2 , and broad resonances characteristic of oligo- or poly(phenylsilane), $(\text{PhSiH})_n$. Allowing the mixture to react over 1 week at room temperature increased the intensity of the broad peaks assigned to $(\text{PhSiH})_n$.

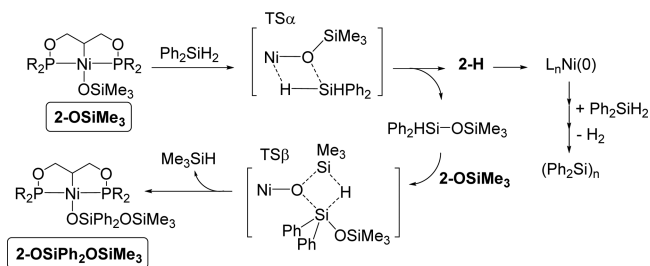
Attempts to isolate **2-H** and the other species A–C were unsuccessful, because the reaction mixture evolved continuously to give multiple species in small quantities; nevertheless, ^1H NMR ([Figure S38](#) for **2-H** and [Figure S41](#) for species C) and GC/MS analyses of these mixtures helped identify two of the nonmetallic species as Ph_2SiH_2 and $\text{PhSiH}_2\text{OSiMe}_3$. That different products observed in the reactions of **2-OSiMe₃** and PhSiH_3 under different conditions, i.e., polymeric materials forming from room temperature reactions and Ph_2SiH_2 from reactions initiated at low temperatures, indicate that redistribution and Si–Si bond formation reactions might occur independently of each other and are promoted by different Ni species. Some evidence in support of this contention was obtained from ^{31}P NMR monitoring of a 1:50 mixture of **2-**

OSiMe₃ and PhSiH₃ at room temperature (Figures S42 and S43): we observed the formation of free ligand (POC_{sp³}HOP, 151 ppm) and *i*-Pr₂PH (−15.8 ppm) in the first hour of the reaction. The free ligand likely arises via reductive elimination of the in situ generated Ni–H species **2-H**, a process observed previously for the analogous species (PC_{sp³}P)NiH,³⁹ whereas *i*-Pr₂PH likely arises from the attack of the hydride moiety on the P–O moiety of (POC_{sp³}OP)NiX.⁴⁰

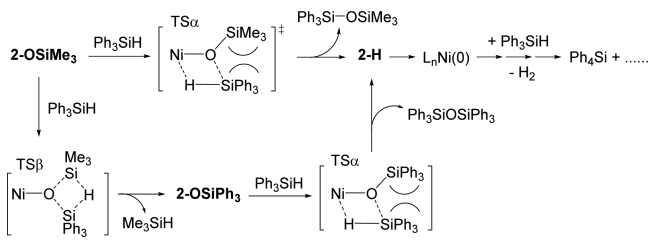
Regardless of the precise mechanism(s) leading to the above side products, their detection in the reaction mixture implies that Ni(0) species are generated in this system and that they might be active in the polymerization reaction. Indirect support for this postulate was furnished by the results of the following experiment. Addition of excess PhSiH₃ to a red solution obtained from stirring Ni(COD)₂ with free protio ligand POC_{sp³}HOP for 1 h at room temperature led to a vigorous evolution of gas and generated polymeric substances as indicated by broad SiH signals at ca. 4.5–4.8 ppm (Figures S44–S47).⁴¹ We conclude, therefore, that the reaction of **2-OSiMe₃** with PhSiH₃ leads initially to **2-H** and that the fate of this intermediate depends on the reaction conditions: at lower temperatures, it is converted to silyl derivatives that promote the redistribution of PhSiH₃, whereas at room temperature **2-H** decomposes to zero-valent species that promote the oligo- or polymerization process (Scheme 6). Given the different types of polymeric substances produced in the reactions promoted by **2-OSiMe₃** and zero-valent species, we speculate that the latter produces linear or cyclic (PhSiH)_{*n*} that are converted to cross-linked poly(phenylsilane) by divalent species **2-X** (in particular when THF is present in the reaction medium).

Mechanistic Proposals Pertaining to Reactivities of 2-OSiMe₃ with Ph₂SiH₂ and Ph₃SiH. By analogy to the above-described observations from the reaction of **2-OSiMe₃** with PhSiH₃, we can propose the reaction schemes illustrated in Schemes 7 and 8 as tentative mechanisms for the analogous

Scheme 7. Proposed Pathways for Reactions of 2-OSiMe₃ with Ph₂SiH₂



Scheme 8. Proposed Pathways for the Reactions of 2-OSiMe₃ with Ph₃SiH



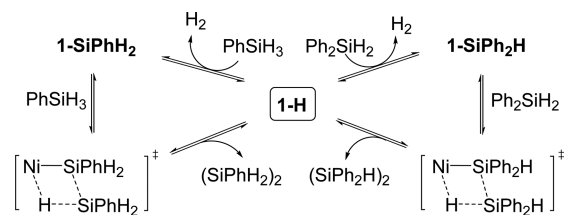
reactions of Ph₂SiH₂ and Ph₃SiH. Thus, the initial reaction between **2-OSiMe₃** and Ph₂SiH₂ generates **2-H** and Ph₂SiHOSiMe₃ via a classical σ -bond metathesis pathway

(TS α in Scheme 7). Decomposition of **2-H** generates zero-valent species that then react with excess monomer to give the observed insoluble red solid, whereas Ph₂SiHOSiMe₃ reacts with residual **2-OSiMe₃** to give the observed siloxide derivative **2-OSiPh₂OSiMe₃** through the unconventional metathesis-like pathway alluded to above (TS β in Scheme 7).

Scheme 8 proposes a similar mechanism for the reaction of **2-OSiMe₃** with Ph₃SiH: the silyl ether Ph₃SiOSiMe₃ and **2-H** are generated via the conventional TS α , and decomposition of the latter generates a zero-valent species much as discussed above for the reactions with PhSiH₃ and Ph₂SiH₂. In this case, however, the zero-valent species does not polymerize Ph₃SiH, leading instead to the redistribution product Ph₄Si. Another difference between the Ph₂SiH₂ and Ph₃SiH reactions is that for the latter case a reaction via the unconventional pathway TS β leads to the formation of **2-OSiPh₃** that reacts further with unreacted Ph₃SiH to give via TS α the symmetrical disilyl ether Ph₃SiOSiPh₃ and **2-H**.

Proposed Mechanisms for the Dehydrogenative Dimerization and Redistribution in the Reactions of 1-OSiMe₃ with Ph_{*n*}SiH_{4-*n*}. As mentioned above, the reaction of **1-OSiMe₃** with PhSiH₃ and Ph₂SiH₂ gave hydrido and silyl derivatives **1-H**, **1-SiPhH₂**, and **1-SiPh₂H** in addition to variable amounts of the silane redistribution products Ph₂SiH₂ and Ph₃SiH and dehydrogenative dimerization products (PhSiH₂)₂^{4a,7a,12,15} and (Ph₂SiH)₂.¹² We have argued above that the new silyl derivatives are generated via concerted, constant-oxidation-state σ -bond metathesis type transition states as opposed to successive oxidative addition/reductive elimination reactions going through Ni^{IV} intermediates. Similar arguments can be advanced to rationalize the formation of the observed disilanes via concerted transition states, as shown in Scheme 9.

Scheme 9. Proposed Transition States for the Dimerization of PhSiH₃ and Ph₂SiH₂



The redistribution-type side reactions, e.g., formation of Ph₂SiH₂ from PhSiH₃ or Ph₃SiH from Ph₂SiH₂, occur quite commonly in the reactions of hydrosilanes with various transition metal species and are thought to proceed via metal-silylene intermediates, M(SiR₂).^{12,42} Metal silylenes are most readily prepared by Lewis acid abstraction of heteroatom-based Si substituents in silyl species M–SiR₂X,^{43,44} but in a number of cases, silylenes have been generated from M(SiHR₂) species via Si-to-M α H migration. Bulk of the silylene species formed via this latter path occur with metals from groups 6 (Mo⁴⁵ and W⁴⁶), 8 (Os⁴⁷), and 9 (Rh⁴⁸ and Ir⁴⁹), but Tilley's group has reported one example of α H migration with a group 10 metal silyl precursor: abstraction of the Me ligand in (dippe)PtMe(Si{Mes}₂H) (dippe = *i*-Pr₂PCH₂)₂, Mes = 2,4,6-Me₃C₆H₂) by B(C₆F₅)₃ generated the silylene(hydride) species [(dippe)PtH(Si{Mes}₂)]⁺.^{50,51}

The above precedents raise the following question: is it reasonable to expect that the silyl derivatives **1-SiPhH₂** and **1-**

SiPh_2H generated in our system lead to Ni–silylene intermediates via αH migrations? First, it is worth noting that Ni complexes bearing nonstabilized silylenes of the type “: SiPh_2 ” or “: SiPhH ” that would result from the proposed αH migrations are unprecedented: to our knowledge, the only examples of unambiguously characterized Ni(silylene) complexes are based on the so-called stable *N*-heterocyclic silylenes that are isolobal to NHC carbenes.^{52,53} Second, Tilley’s group has shown that the above-mentioned conversion of the Pt–silyl to Pt(silylene) requires a Lewis acid generated vacant coordination site in a 14-electron intermediate; indeed, the charge-neutral, four-coordinate species $(\text{dippe})\text{PtMe}(\text{Si}\{\text{Mes}\}_2\text{H})$ does not convert to a silylene species in the absence of $\text{B}(\text{C}_6\text{F}_5)_3$ even when it is heated to 110 °C for 2 weeks.^{50,54} Finally, a report by Iluc and Hillhouse⁵⁵ has established that αH migrations might be difficult with Ni^{II} even when it features a vacant coordination site within a cationic 14-electron intermediate: one-electron oxidation of the Ni(I) silyl complex $(\text{dtbpe})\text{Ni}(\text{Si}\{\text{Mes}\}_2\text{H})$ ($\text{dtbpe} = \{t\text{-Bu}_2\text{PCH}_2\}_2$) generated $[(\text{dtbpe})\text{Ni}(\mu\text{-H})(\text{SiAr}_2)]^+$ that can be viewed as a protonated silylene or the arrested form of a αH migration from Si to Ni induced by the $\text{Ni}^{\text{I}} \rightarrow \text{Ni}^{\text{II}}$ oxidation. These precedents suggest that the silyl species generated in our system are unlikely to lead to the silylene intermediates “(POCOP)Ni(H)(SiR₂)” given that our reactions were conducted in the absence of Lewis acids and oxidants. Note also that there is no evidence in the solid structures of **1-SiPhH₂** and **1-SiPh₂H** (vide supra) for agostic Ni–H interactions that might foretell the predisposition of these species to αH migrations.

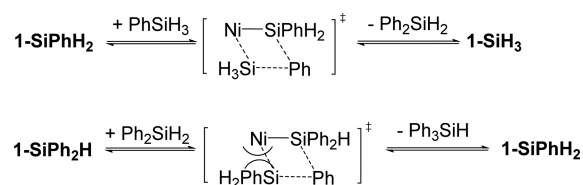
The above arguments against the involvement of silylene intermediates in our system indicate that a different mechanism must be operative for the facile redistribution reactions discussed earlier. Close inspection of the products arising from redistribution and dimerization reactions initiated by **1-OSiMe₃** gave us a useful clue for answering this question: the reaction with PhSiH_3 gave comparable quantities of the two types of products ($(\text{PhH}_2\text{Si})_2/\text{Ph}_2\text{SiH}_2 \approx 1.2:1.0$; Figure S48), whereas the reaction with Ph_2SiH_2 favored the Si–Si bond formation pathway ($(\text{Ph}_2\text{HSi})_2/\text{Ph}_3\text{SiH} \approx 3.0:1.0$; Figure S49). These ratios appear to suggest that steric factors are more consequential for the redistribution pathway and might indicate that Si substituents might be in close contact with the Ni center. The crucial importance of steric factors, originating from both the Si substituents on the hydrosilane and P substituent(s) of the pincer ligand, have been clearly demonstrated by Waterman’s recent report on the competitive redistribution and dehydrogenative coupling of hydrosilanes.¹²

The observed impact of hydrosilane sterics in the present context can be reconciled with a simple mechanistic proposal that provides an alternative to the silylene pathway alluded to above. This proposal involves a slightly different σ -bond metathesis type transition state in which the Ni center interacts with the silyl end of the approaching hydrosilane (Scheme 10). Thus, the in situ formed silyl derivatives would react with phenyl(hydrosilanes) via two different concerted pathways leading to disilanes via Si–H bond rupture and Si–Si bond formation (Scheme 9) or redistribution products via Si–C bond rupture and formation (Scheme 10).

CONCLUSIONS

This study has validated our strategy based on using siloxide precursors to shed light on the complex reactivities of divalent nickel with hydrosilanes. The detection, at various stages of the

Scheme 10. Proposed Transition States for the Redistribution of PhSiH_3 and Ph_2SiH_2



investigated reactions, of $\text{Me}_3\text{SiO-}$ and $\text{Ph}_n\text{Si}_{3-n}\text{O-}$ -containing disilyl ethers as well as new Ni–siloxide derivatives has revealed new reaction pathways that might lead to development of new Ni-promoted synthesis processes. In particular, the proposed $2s + 2s$ rearrangements occurring between siloxide moieties and sterically encumbered hydrosilanes or disilyl ethers (without involving the Ni center) should inspire new synthetic avenues.

The different reactivities promoted by our $\text{POC}_{\text{sp}^3}\text{OP-}$ and $\text{POC}_{\text{sp}^3}\text{OP-Ni}$ complexes underline the importance of ligand backbone in favoring one course of reaction over another, in this case hydrosilane dimerization and redistribution over dehydrogenative oligo- and polymerization. The evidence presented above for the involvement of zero-valent Ni species in reaction settings that lead to polysilanes also implies that the latter result from stepwise pathways that shuttle Ni^0 and Ni^{II} intermediates.⁵⁶ In contrast, the reactivities of $\text{Ph}_n\text{SiH}_{4-n}$ with divalent hydrido and silyl derivatives lead to dimerization and redistribution reactions through concerted, constant-oxidation-state reactions that exchange Ni–X, Si–H, and Si–C bonds. The subtle balance between these two different outcomes appears to be governed by two factors: the pincer ligand backbone and the steric bulk of Si substituents.

Future efforts will be directed toward application of the observed new reactivities with Ni–siloxide derivatives as well as testing the generality of these reactivities with analogous precursors such as Ni–thiolates and Ni–amides.

EXPERIMENTAL SECTION

General. All manipulations were carried out under nitrogen using standard Schlenk procedures and a dry box. Solvents were dried by passage over molecular sieves contained in MBRAUN systems. Phenylsilane (Aldrich) was dried over CaH_2 and distilled prior to use; diphenylsilane (Aldrich) was dried over 4 Å molecular sieves. Triphenylsilane was used without further purification. Literature procedures were employed to prepare $(\text{POC}_{\text{sp}^3}\text{OP})\text{NiCl}$ (**1-Cl**)⁵⁷ and $(\text{POC}_{\text{sp}^3}\text{OP})\text{NiBr}$ (**2-Br**).^{10b,c} A Bruker AV400 NMR spectrometer was used for recording ^1H (400 MHz), ^{31}P (161.9 MHz), and ^{13}C (100.56 MHz) NMR spectra. Unless otherwise specified, the NMR spectra were recorded at room temperature (ca. 25 °C), and the chemical shift values are reported in ppm (δ) and referenced internally to the residual solvent signals (^1H : 7.15 and ^{13}C : 128.06 ppm for C_6D_6) or externally (^{31}P , H_3PO_4 in D_2O , $\delta = 0$). Coupling constants are reported in hertz. The elemental analyses were carried out by the Laboratoire d’Analyse Élémentaire, Département de Chimie, Université de Montréal. The GPC analyses were carried out on a Waters GPC system equipped with a refractive index detector calibrated with polystyrene standards in THF. Average molecular weights were calculated relative to those of polystyrene standards.

Synthesis of $(\text{POC}_{\text{sp}^3}\text{OP})\text{Ni}(\text{SiPhH}_2)$, **1-SiPhH₂.** To a room-temperature solution of **1-OSiMe₃** (150 mg, 0.307 mmol) in toluene (20 mL) was added PhSiH_3 (376 μL , 3.05 mmol), and the mixture was stirred at room temperature and the head gas purged occasionally with pure N_2 gas to remove the in situ generated gases. Analysis of the reaction mixture after 8 days of stirring and purging showed that very little of Guan’s hydride **1-H** was left. Pumping all the volatiles and extraction of the solid residue with *n*-hexane (15 mL) gave a yellowish

mixture, which was filtered, concentrated to 0.5 mL, and stored at $-40\text{ }^{\circ}\text{C}$ for 1 week to give the target complex as yellow crystals (32 mg, 21%). ^1H NMR (δ , C_6D_6) 1.24 (ps sextet, $^3J_{\text{HH}} = 6.9$, $^3J_{\text{HH}} = 8.6$, $^{\nu}J_{\text{HP}} = 7.4$, 24H, $\text{PCH}(\text{CH}_3)_2$), 2.17 (sept, $^3J_{\text{HH}} = 7.0$, 4H, $\text{PCH}(\text{CH}_3)_2$), 4.74 (t, $^3J_{\text{HP}} = 7.5$, 2H, SiH_2), 6.83 (d, $^3J_{\text{HH}} = 7.8$, 2H, Ar-H), 7.02 (t, $^3J_{\text{HH}} = 7.8$, 2H, Ar-H), 7.11–7.21 (m, 2H, Ar-H), 7.82 (m, 2H, Ar-H). $^{13}\text{C}\{^1\text{H}\}$ NMR (δ , C_6D_6) 17.05 (s, 4C, $\text{PCH}(\text{CH}_3)_2$), 18.25 ($^{\nu}$, $^{\nu}J_{\text{PC}} = 2.6$, 4C, $\text{PCH}(\text{CH}_3)_2$), 29.12 ($^{\nu}$, $^{\nu}J_{\text{PC}} = 13.9$, 4C, $\text{PCH}(\text{CH}_3)_2$), 104.65 (t, $J_{\text{PC}} = 6.3$, 2C, C_{meta}), 125.66 (s, Ar-C), 129.30 (s, Ar-C), 130.27 (s, Ar-C), 136.27 (s, Ar-C), 142.29 (s, Ar-C), 142.93 (t, $J_{\text{PC}} = 15.9$, Ar-C), 167.33 (t, $J_{\text{PC}} = 9.2$, 2C, C_{ortho}). $^{31}\text{P}\{^1\text{H}\}$ NMR (δ , 25 $^{\circ}\text{C}$, 162 M, C_6D_6) 201.30 (s). Anal. Calcd for $\text{C}_{24}\text{H}_{38}\text{O}_2\text{P}_2\text{SiNi}$ (507.28) C, 56.82; H, 7.55. Found: C, 57.35; H, 7.66.

Synthesis of $(\text{POC}_{\text{sp}}\text{OP})\text{Ni}(\text{SiPh}_2\text{H})$, **1-SiPh₂H.** To a room-temperature solution of **1-OSiMe₃** (120 mg, 0.245 mmol) in toluene (20 mL) was added Ph_2SiH_2 (455 μL , 2.45 mmol), and the mixture was stirred while being heated at $90\text{ }^{\circ}\text{C}$ for 1 week. During this period, the head gas was purged occasionally with pure N_2 gas to remove the in situ generated volatiles. Evaporation of the final mixture and extraction of the solid residues with *n*-hexane (15 mL) followed by filtration gave a yellow solution, which was concentrated to 1 mL and stored at $-40\text{ }^{\circ}\text{C}$ for 1 week to give a crop of yellowish crystals of the target complex as well as white crystals identified as Ph_3SiH . The yellowish crystals were carefully separated from the mixture and recrystallized to give analytically pure samples of the target complex (44 mg, 25%). ^1H NMR (δ , C_6D_6) 1.02 (dt $^{\nu}$, $^3J_{\text{HH}} = 9.4$, $^{\nu}J_{\text{HP}} = 7.6$, 12H, $\text{PCH}(\text{CH}_3)_2$), 1.11 (dt $^{\nu}$, $^3J_{\text{HH}} = 7.0$, $^{\nu}J_{\text{HP}} = 7.0$, 12H, $\text{PCH}(\text{CH}_3)_2$), 2.07 (sept, $^3J_{\text{HH}} = 7.1$, 4H, $\text{PCH}(\text{CH}_3)_2$), 5.43 (t, $^3J_{\text{HP}} = 12.5$, 1H, SiH), 6.84 (d, $^3J_{\text{HH}} = 7.8$, 2H, Ar-H), 7.04 (t, $^3J_{\text{HH}} = 7.8$, 1H, Ar-H), 7.18–7.21 (m, 4H, Ar-H), 7.83 (d, $^3J_{\text{HH}} = 6.5$, 4H, Ar-H). Note that two H atoms were overlapped by residual solvent resonance. $^{13}\text{C}\{^1\text{H}\}$ NMR (δ , C_6D_6) 16.84 (s, 4C, $\text{PCH}(\text{CH}_3)_2$), 18.41 ($^{\nu}$, $^{\nu}J_{\text{PC}} = 2.3$, 4C, $\text{PCH}(\text{CH}_3)_2$), 29.21 ($^{\nu}$, $^{\nu}J_{\text{PC}} = 13.6$, 4C, $\text{PCH}(\text{CH}_3)_2$), 104.51 (t, $J_{\text{PC}} = 6.2$, C_{meta}), 127.50 (s, Ar-C), 130.35 (s, Ar-C), 137.12 (s, Ar-C), 142.71 (t, $J_{\text{PC}} = 14.8$), 144.20 (s, Ar-C), 167.30 (t, $J_{\text{PC}} = 9.0$, C_{ortho}). $^{31}\text{P}\{^1\text{H}\}$ NMR (δ , C_6D_6) 199.70 (s). Anal. Calcd for $\text{C}_{30}\text{H}_{42}\text{O}_2\text{P}_2\text{SiNi}$ (583.37) C, 61.76; H, 7.26. Found: C, 62.00; H, 7.40.

Synthesis of $(\text{POC}_{\text{sp}}\text{OP})\text{Ni}(\text{OSiPh}_2\text{OSiMe}_3)$, **2-OSiPh₂OSiMe₃.** To a room-temperature solution of **2-OSiMe₃** (230 mg, 0.505 mmol) in toluene (10 mL) was added dropwise Ph_2SiH_2 (93 μL , ca. 0.5 mmol), and the mixture stirred at room temperature overnight. Removal of all volatiles followed by extraction of the solid residues with *n*-hexane (15 mL) gave a yellow solution that was concentrated to 0.5 mL and stored at $-40\text{ }^{\circ}\text{C}$ for 2 days to give the target complex as yellow crystals (110 mg, 34%). ^1H NMR (δ , C_6D_6) 0.12 (s, 9H, SiMe_3), 1.21 (dt $^{\nu}$, $^3J_{\text{HH}} = 6.9$ and $^{\nu}J_{\text{HP}} = 5.9$, 6H, $\text{PCH}(\text{CH}_3)_2$), 1.24–1.32 (m, 12H, $\text{PCH}(\text{CH}_3)_2$), 1.46 (dt $^{\nu}$, $^3J_{\text{HH}} = 9.3$ and $^{\nu}J_{\text{HP}} = 7.4$, 6H, $\text{PCH}(\text{CH}_3)_2$), 1.83 (sept, $^3J_{\text{HH}} = 7.2$, 2H, $\text{PCH}(\text{CH}_3)_2$), 1.97 (sept, $^3J_{\text{HH}} = 7.2$, 2H, $\text{PCH}(\text{CH}_3)_2$), 2.45 (m, 1H, CH_2CHCH_2), 3.13 (dd, $^3J_{\text{HH}} = 9.2$, $^3J_{\text{HH}} = 6.7$, 2H, CH_2CHCH_2), 3.21–3.33 (m, 2H, CH_2CHCH_2), 7.19–7.25 (m, 2H, Ar-H), 7.27–7.31 (m, 4H, Ar-H), 7.85–7.88 (m, 4H, Ar-H). $^{13}\text{C}\{^1\text{H}\}$ NMR (δ , C_6D_6) 2.41 (s, 3C, SiMe_3), 16.28 (s, 2C, $\text{PCH}(\text{CH}_3)_2$), 16.99 (s, 2C, $\text{PCH}(\text{CH}_3)_2$), 18.11 ($^{\nu}$, $^{\nu}J_{\text{PC}} = 3.8$, 2C, $\text{PCH}(\text{CH}_3)_2$), 19.00 ($^{\nu}$, $^{\nu}J_{\text{PC}} = 3.4$, 2C, $\text{PCH}(\text{CH}_3)_2$), 27.59 ($^{\nu}$, $^{\nu}J_{\text{PC}} = 11.5$, 2C, $\text{PCH}(\text{CH}_3)_2$), 28.50 ($^{\nu}$, $^{\nu}J_{\text{PC}} = 9.3$, 2C, $\text{PCH}(\text{CH}_3)_2$), 42.80 (t, $J_{\text{PC}} = 13.5$, 1C, CH-Ni), 76.60 ($^{\nu}$, $^{\nu}J_{\text{PC}} = 7.8$, 2C CH_2CHCH_2), 127.24 (s, Ar-C), 135.23 (s, Ar-C), 142.77 (s, Ar-C). $^{31}\text{P}\{^1\text{H}\}$ NMR (C_6D_6) 176.77 (s). Anal. Calcd for $\text{C}_{30}\text{H}_{52}\text{O}_4\text{P}_2\text{Si}_2\text{Ni}$ (653.54) C, 55.13; H, 8.02. Found: C, 54.79; H, 8.26.

NMR Monitoring of Reaction of **2-OSiMe₃ with **PhSiH₃**.** A PTFE-capped NMR tube was charged with **2-OSiMe₃** (9 mg, 0.02 mmol) and 0.7 mL of toluene- d_8 , and the mixture was cooled to $-70\text{ }^{\circ}\text{C}$. Excess PhSiH_3 (17 mg, 0.016 mmol) was added at this temperature, and the NMR tube was promptly transferred into the precooled probe of the NMR instrument. ^1H and ^{31}P NMR spectra were recorded over ca. 10 min before warming the sample to ca. $-55\text{ }^{\circ}\text{C}$, recording new spectra, and repeating this process at $15\text{ }^{\circ}\text{C}$

intervals. The overall observations of this experiment are described in the **Results and Discussion** section. Provided here are partial data for the tentatively identified products generated in situ. $(\text{POC}_{\text{sp}}\text{OP})\text{Ni}(\text{H})$, **2-H**: ^1H NMR (δ , $-70\text{ }^{\circ}\text{C}$, 500 M, $\text{C}_7\text{-D}_8$) -9.06 (t, $J_{\text{HP}} = 57.3$, 1H, NiH), 1.16–1.26 (m, 24H, $\text{PCH}(\text{CH}_3)_2$), 1.90 (sept, $J_{\text{HH}} = 6.8$, 2H, $\text{PCH}(\text{CH}_3)_2$), 2.00 (sept, $J_{\text{HH}} = 6.7$, 2H, $\text{PCH}(\text{CH}_3)_2$), 2.84 (m, 1H, $J_{\text{HH}} = 9.3$, CH_2CHCH_2), 3.37 (m, 0.5H, CH_2CHCH_2), 3.37 (dd, $J_{\text{HH}} = 11.7$, $J_{\text{HH}} = 8.9$, 2H, CH_2CHCH_2), 3.85 (m, 0.5H, CH_2CHCH_2), 4.39 (m, 0.5H, CH_2CHCH_2), 4.65 (m, 0.5H, CH_2CHCH_2). $^{31}\text{P}\{^1\text{H}\}$ NMR (δ , $-70\text{ }^{\circ}\text{C}$, 202 M, $\text{C}_7\text{-D}_8$) 200.44 (s). **PhSiH₂OSiMe₃**: ^1H NMR (δ , $-70\text{ }^{\circ}\text{C}$, 500 M, $\text{C}_7\text{-D}_8$) 0.11 (s, 9H, $\text{Si}(\text{CH}_3)_3$), 5.42 (2H, SiH_2). $(\text{POC}_{\text{sp}}\text{OP})\text{NiOSiR}_3$, **2-OSiR₃** (species C): $^{31}\text{P}\{^1\text{H}\}$ NMR (δ , 25 $^{\circ}\text{C}$, 202 M, $\text{C}_7\text{-D}_8$) 177.6 (s). For ^1H NMR, see **Figure S41**.

General Procedure for Polymerization of **PhSiH₃.** Working inside a glovebox and at room temperature, 200 equiv of PhSiH_3 was added to a Schlenk flask containing **2-OSiMe₃** (12 mg, 0.026 mmol) either in solid form (neat reaction) or as a concentrated solution in C_6H_6 (1 mL). Vigorous effervescence was observed upon mixing. The reaction vessel was sealed with a septum, brought out of the glovebox, and connected to a double-manifold Schlenk line. With the reaction vessel under positive pressure of nitrogen, a small syringe needle was installed on the septum to remove volatiles in the head gas. The mixture was stirred at room temperature with occasional purging of the head gas overnight, and the solid products that formed in the vessel were isolated as follows: dry THF (3 mL) was added to the mixture and stirred for 3 h before concentrating under vacuum. After all volatiles were removed, hexane (10 mL) and acetonitrile (5 mL) were sequentially added to wash the solid residues. This procedure gave a white solid, which was dried overnight under vacuum and identified as cross-linked poly(phenylsilane) (ca. 60–70% yield).

Phenylsilane Oligomerization/Polymerization Test Mediated by the Combination of $\text{POC}_{\text{sp}}\text{HOP}$ and $\text{Ni}(\text{COD})_2$. Addition of 10 equiv of $\text{POC}_{\text{sp}}\text{HOP}$ ligand (310 mg, 1 mmol) to an NMR tube containing $\text{Ni}(\text{COD})_2$ (28 mg, 0.1 mmol) turned the original yellow color of $\text{Ni}(\text{COD})_2$ to red. This sample was allowed to stand for 1 day; then, PhSiH_3 (430 mg, ca. 4 mmol) was added, which generated a vigorous evolution of gas upon contact. NMR monitoring of the sample showed a broad Si–H resonance at 4.5–4.8 ppm, indicating the formation of $(\text{SiPhH})_n$.

■ ASSOCIATED CONTENT

● Supporting Information

Complete details of the X-ray analyses reported herein have been deposited at The Cambridge Crystallographic Data Center (CCDC nos.: 1421313 for **1-SiPhH₂**, 1421314 for **1-SiPh₂H**, and 1421312 for **2-OSiPh₂OSiMe₃**). This data can be obtained free of charge via http://www.ccdc.cam.ac.uk/data_request/cif, by e-mailing data_request@ccdc.cam.ac.uk, or by contacting The Cambridge Crystallographic Data Centre, 12 Union Road, Cambridge CD2 1EZ, United Kingdom, fax: + 44 1223 336033. The Supporting Information is available free of charge on the ACS Publications website at DOI: 10.1021/jacs.5b10066.

Crystallographic information files for **1-SiPhH₂**, **1-SiPh₂H**, and **2-OSiPh₂OSiMe₃**. (**CIF**)

General information about crystallographic work, crystal data and collection/refinement parameters, sample NMR spectra, and GC/MS traces. (**PDF**)

■ AUTHOR INFORMATION

Corresponding Author

*E-mail: zargarian.davit@umontreal.ca.

Notes

The authors declare no competing financial interest.

ACKNOWLEDGMENTS

We gratefully acknowledge the financial support provided by NSERC of Canada (Discovery grant to D.Z.), FRQNT (Group Research grant to D.Z.), and Université de Montréal. We are also grateful to Professors R. Waterman and H. Schaper for valuable discussions; to Mrs. Berline Mougang-Soumé for collecting the X-ray data for the compound 2-OSiPh₂OSiMe₃ and preliminary attempts at solving it; to Mrs. Francine Bélanger-Gariépy for her expert help in fully solving the latter structure; to the reviewer of our manuscript for urging us to recognize and explicitly comment on the possible involvement of (a) Ni particles in the polymerization reactions and (b) Si–H bond activation mechanisms involving oxidative addition as opposed to constant-oxidation-state σ -bond-metathesis steps.

REFERENCES

(1) For selected reviews on polysilanes and their optical and semiconducting properties, see (a) West, R. J. *Organomet. Chem.* **1986**, *300*, 327–331. (b) Miller, R. D.; Michl, J. *Chem. Rev.* **1989**, *89*, 1359–1410. (c) West, R.; Menescal, R.; Asuke, T.; Eveland, J. J. *Inorg. Organomet. Polym.* **1992**, *2*, 29–45. (d) Naito, M.; Fujiki, M. *Soft Matter* **2008**, *4*, 211–223.

(2) For a selection of primary reports and reviews on catalytic dehydrogenative polymerization of hydrosilanes, see (a) Aitken, C. T.; Harrod, J.; Samuel, F. E. J. *Organomet. Chem.* **1985**, *279*, C11–C13. (b) Aitken, C. T.; Harrod, J.; Samuel, F. E. J. *Am. Chem. Soc.* **1986**, *108*, 4059–4066. (c) Aitken, C.; Harrod, J. F.; Samuel, E. *Can. J. Chem.* **1986**, *64*, 1677–1679. (d) Aitken, C.; Harrod, J. F.; Gill, U. S. *Can. J. Chem.* **1987**, *65*, 1804–1809. (e) Harrod, J. F.; Yun, S. D. *J. Am. Chem. Soc.* **1989**, *111*, 8043–8044. (f) Harrod, J. F.; Yun, S. D. *J. Am. Chem. Soc.* **1989**, *111*, 8043–8044. (g) Tilley, T. D. *Comments Inorg. Chem.* **1990**, *10*, 37–51. (h) Hengge, E.; Weinberger, M. J. *Organomet. Chem.* **1992**, *433*, 21–34. (i) Yamashita, H.; Tanaka, M. *Bull. Chem. Soc. Jpn.* **1995**, *68*, 403–419. (j) Corey, J. Y. *Adv. Organomet. Chem.* **2004**, *51*, 1–52.

(3) (a) Yamamoto, K.; Okinoshima, H.; Kumada, M. *J. Organomet. Chem.* **1971**, *27*, C31–C32. (b) Curtis, M. D.; Epstein, P. S. *Adv. Organomet. Chem.* **1981**, *19*, 213–255. (c) Fryzuk, M. D.; Rosenberg, L.; Rettig, S. J. *Inorg. Chim. Acta* **1994**, *222*, 345–364. (d) Hashimoto, H.; Tobita, H.; Ogino, H. *J. Organomet. Chem.* **1995**, *499*, 205–211. (e) Radu, N. S.; Hollander, F. J.; Tilley, T. D.; Rheingold, A. L. *Chem. Commun.* **1996**, *21*, 2459–2460. (f) Rosenberg, L.; Davis, C. W.; Yao, J. J. *Am. Chem. Soc.* **2001**, *123*, 5120–5121. (g) Park, S.; Kim, B. G.; Göttker-Schnetmann, I.; Brookhart, M. *ACS Catal.* **2012**, *2*, 307–316.

(4) (a) Woo, H. G.; Walzer, J. F.; Tilley, T. D. *J. Am. Chem. Soc.* **1992**, *114*, 7047–7055. (b) Hengge, E.; Weinberger, M. J. *Organomet. Chem.* **1993**, *443*, 167–173. (c) Ziegler, T.; Folga, E. J. *Organomet. Chem.* **1994**, *478*, 57–65. (d) Rosenberg, L. *Macromol. Symp.* **2003**, *196*, 347–353. (e) Spencer, M. D.; Shelby, Q. D.; Girolami, G. S. *J. Am. Chem. Soc.* **2007**, *129*, 1860–1861. (f) Waterman, R. *Organometallics* **2013**, *32*, 7249–7263.

(5) (a) Johnson, C. E.; Eisenberg, R. *J. Am. Chem. Soc.* **1985**, *107*, 6531–6540. (b) Shintani, K.; Ooi, O.; Mori, A.; Kawakami, Y. *Polym. Bull.* **1997**, *38*, 1–5. (c) Aizenberg, M.; Ott, J.; Elsevier, C. J.; Milstein, D. *J. Organomet. Chem.* **1998**, *551*, 81–92. (d) Diversi, P.; Marchetti, F.; Ermini, V.; Matteoni, S. *J. Organomet. Chem.* **2000**, *593*–594, 154–160. (e) Baumgartner, T.; Wilk, W. *Org. Lett.* **2006**, *8*, 503–506. (f) Itazaki, M.; Ueda, K.; Nakazawa, H. *Angew. Chem., Int. Ed.* **2009**, *48*, 3313–3316.

(6) (a) Boudjouk, P.; Rajkumar, A. B.; Parker, W. L. *J. Chem. Soc., Chem. Commun.* **1991**, 245–246. (b) Smith, E. E.; Du, G.; Fanwick, P. E.; Abu-Omar, M. M. *Organometallics* **2010**, *29*, 6527–6533. (c) Tanabe, M.; Takahashi, A.; Fukuta, T.; Osakada, K. *Organometallics* **2013**, *32*, 1037–1043.

(7) (a) Fontaine, F.-G.; Zargarian, D. *Organometallics* **2002**, *21*, 401–408. (b) Fontaine, F.-G.; Zargarian, D. *J. Am. Chem. Soc.* **2004**, *126*,

8786–8794. (c) Chen, Y.; Sui-Seng, C.; Boucher, S.; Zargarian, D. *Organometallics* **2005**, *24*, 149–155.

(8) (a) Fontaine, F.-G.; Kadkhodazadeh, T.; Zargarian, D. *Chem. Commun.* **1998**, 1253–1254. (b) Groux, L. F.; Zargarian, D. *Organometallics* **2001**, *20*, 3811–3817. (c) Fontaine, F.-G.; Nguyen, R.-V.; Zargarian, D. *Can. J. Chem.* **2003**, *81*, 1299–1306. (d) Gareau, D.; Sui-Seng, C.; Groux, L. F.; Brisse, F.; Zargarian, D. *Organometallics* **2005**, *24*, 4003–4013. (e) Sui-Seng, C.; Castonguay, A.; Chen, Y.; Gareau, D.; Groux, L. F.; Zargarian, D. *Top. Catal.* **2006**, *37*, 81–90. (f) Chen, Y.; Zargarian, D. *Can. J. Chem.* **2009**, *87*, 280–287.

(9) Zargarian, D.; Castonguay, A.; Spasyuk, D. M.; van Koten, G.; Milstein, D. *Top. Organomet. Chem.* **2013**, *40*, 131–173.

(10) For a selection of reports on the stoichiometric and catalytic reactivities of POCOP–Ni complexes, see (a) Gómez-Benitez, V.; Baldovino-Pantaleon, O.; Herrera-Álvarez, C.; Toscano, R. A.; Morales-Morales, D. *Tetrahedron Lett.* **2006**, *47*, 5059–5062. (b) Pandarus, V.; Zargarian, D. *Chem. Commun.* **2007**, 978–980. (c) Pandarus, V.; Zargarian, D. *Organometallics* **2007**, *26*, 4321–4334. (d) Morales-Morales, D. *Mini-Rev. Org. Chem.* **2008**, *5*, 141–152. (e) Castonguay, A.; Spasyuk, D.; Madern, N.; Beauchamp, A. L.; Zargarian, D. *Organometallics* **2009**, *28*, 2134–2141. (f) Solano-Prado, M. A.; Estudiante-Negrete, F.; Morales-Morales, D. *Polyhedron* **2010**, *29*, 592–600. (g) Chakraborty, S.; Zhang, J.; Krause, J. A.; Guan, H. *J. Am. Chem. Soc.* **2010**, *132*, 8872–8873. (h) Zhang, J.; Medley, C. M.; Krause, J. A.; Guan, H. *Organometallics* **2010**, *29*, 6393–6401. (i) Salah, A.; Zargarian, D. *Dalton Trans.* **2011**, *40*, 8977–8985. (j) Lefèvre, X.; Durieux, G.; Lesturgez, S.; Zargarian, D. *J. Mol. Catal. A: Chem.* **2011**, *335*, 1–7. (k) Lefèvre, X.; Spasyuk, D. M.; Zargarian, D. *J. Organomet. Chem.* **2011**, *696*, 864–870. (l) Salah, A.; Offenstein, C.; Zargarian, D. *Organometallics* **2011**, *30*, 5352–5364. (m) Chakraborty, S.; Zhang, J.; Patel, Y. J.; Krause, J. A.; Guan, H. *Inorg. Chem.* **2013**, *52*, 37–47. (n) Chakraborty, S.; Patel, Y. J.; Krause, J. A.; Guan, H. *Angew. Chem., Int. Ed.* **2013**, *52*, 7523–7526. (o) Vabre, B.; Petiot, P.; Declercq, R.; Zargarian, D. *Organometallics* **2014**, *33*, 5173–5184.

(11) (a) Hao, J.; Mougang-Soumé, B.; Vabre, B.; Zargarian, D. *Angew. Chem., Int. Ed.* **2014**, *53*, 3218–3222. (b) Hao, J.; Vabre, B.; Mougang-Soumé, B.; Zargarian, D. *Chem. - Eur. J.* **2014**, *20*, 12544–12552. (c) Hao, J.; Vabre, B.; Zargarian, D. *Organometallics* **2014**, *33*, 6568–6576.

(12) Mucha, N. T.; Waterman, R. *Organometallics* **2015**, *34*, 3865–3872.

(13) Chakraborty, S.; Krause, J. A.; Guan, H. *Organometallics* **2009**, *28*, 582–586.

(14) It should be noted that these reaction mixtures were purged sporadically to remove the volatiles (presumably H₂ and SiH₄) from the head gas and drive the reaction forward.

(15) (a) Aitken, C.; Barry, J.-P.; Gauvin, F.; Harrod, J. F.; Malek, A.; Rousseau, D. *Organometallics* **1989**, *8*, 1732–1736. (b) Wang, R.; Groux, L. F.; Zargarian, D. *Organometallics* **2002**, *21*, 5531–5539.

(16) Crystal data for Ph₃SiOSiPh₃ (oxo-bis(triphenyl)silicon): triclinic P $\bar{1}$, $a = 8.5563$, $b = 9.4878$, $c = 10.9724$, $\alpha = 96.051$, $\beta = 111.776$, $\gamma = 113.276$, and $V = 725.94$ Å³. See Kooijman, H.; Spek, A. L.; Nijbacker, T.; Lammertsma, K. Private Communication to the Cambridge Structural Database, 1999 (CCDC 135217).

(17) Adhikari, D.; Pink, M.; Mindiola, D. J. *Organometallics* **2009**, *28*, 2072–2077.

(18) (a) Marciniak, B.; Krzyżanowski, P. *J. Organomet. Chem.* **1995**, *493*, 261–266. (b) Kownacki, I.; Kubicki, M.; Marciniak, B. *Polyhedron* **2001**, *20*, 3015–3018. (c) MacBeth, C. E.; Thomas, J. C.; Betley, T. A.; Peters, J. C. *Inorg. Chem.* **2004**, *43*, 4645–4662. (d) Hubert-Pfalzgraf, L. G.; Touati, N.; Pasko, S. V.; Vaissermann, J.; Abrutis, A. *Polyhedron* **2005**, *24*, 3066–3073. (e) Huang, D.; Deng, L.; Sun, J.; Holm, R. H. *Inorg. Chem.* **2009**, *48*, 6159–6166.

(19) (a) Pandarus, V.; Castonguay, A.; Zargarian, D. *Dalton Trans.* **2008**, 4756–4761. (b) Salah, A. B.; Zargarian, D. *Dalton Trans.* **2011**, *40*, 8977–8985. (c) Lefèvre, X.; Durieux, G.; Lesturgez, S.; Zargarian, D. *J. Mol. Catal. A: Chem.* **2011**, *335*, 1–7. (d) Lefèvre, X.; Spasyuk, D. M.; Zargarian, D. *J. Organomet. Chem.* **2011**, *696*, 864–870. (e) Salah, A. B.; Offenstein, C.; Zargarian, D. *Organometallics* **2011**, *30*, 5352–

5364. (f) Vabre, B.; Lambert, M. L.; Petit, A.; Ess, D. H.; Zargarian, D. *Organometallics* **2012**, *31*, 6041–6053. (g) Vabre, B.; Spasyuk, D. M.; Zargarian, D. *Organometallics* **2012**, *31*, 8561–8570.
- (20) (a) Lin, Z. *Chem. Soc. Rev.* **2002**, *31*, 239–245. (b) Schneider, J. *J. Angew. Chem., Int. Ed. Engl.* **1996**, *35*, 1068–1075.
- (21) (a) Bierschenk, T. R.; Guerra, M. A.; Juhlke, T. J.; Larson, S. B.; Lagow, R. J. *J. Am. Chem. Soc.* **1987**, *109*, 4855–4860. (b) Choe, S.-B.; Schneider, J. J.; Klabunde, K. J.; Radonovich, L. J.; Ballintine, T. A. *J. Organomet. Chem.* **1989**, *376*, 419–439. (c) Fischer, R. A.; Nlate, S.; Herdtweck, E. *Angew. Chem., Int. Ed. Engl.* **1996**, *35*, 1861–1863. (d) Gehrhuis, B.; Hitchcock, P. B.; Lappert, M. F.; Maciejewski, H. *Organometallics* **1998**, *17*, 5599–5601. (e) Kang, Y.; Lee, J.; Kong, Y. K.; Kang, S. O.; Ko, J. *Chem. Commun.* **1998**, 2343–2344. (f) Shimada, S.; Rao, M. L. N.; Tanaka, M. *Organometallics* **1999**, *18*, 291–293. (g) Maciejewski, H.; Marciniak, B.; Kownacki, I. *J. Organomet. Chem.* **2000**, *597*, 175–181. (h) Schmedake, T. A.; Haaf, M.; Paradise, B. J.; Powell, D.; West, R. *Organometallics* **2000**, *19*, 3263–3265. (i) Iluc, V. M.; Hillhouse, G. L. *Tetrahedron* **2006**, *62*, 7577–7582. (j) Iluc, V. M.; Hillhouse, G. L. *J. Am. Chem. Soc.* **2010**, *132*, 11890–11892.
- (22) (a) Rosenfield, S. G.; Wong, M. L. Y.; Stephan, D. W.; Mascharak, P. K. *Inorg. Chem.* **1987**, *26*, 4119–4122. (b) Ohtsu, H.; Tanaka, K. *Inorg. Chem.* **2004**, *43*, 3024–3030. (c) Abe, Y.; Akao, H.; Yoshida, Y.; Takashima, H.; Tanase, T.; Mukai, H.; Ohta, K. *Inorg. Chim. Acta* **2006**, *359*, 3147–3155. (d) Liang, L.-C.; Chien, P.-S.; Lee, P.-Y.; Lin, J.-M.; Huang, Y.-L. *Dalton Trans.* **2008**, 3320–3327. (e) Wiese, S.; Kapoor, P.; Williams, K. D.; Warren, T. H. *J. Am. Chem. Soc.* **2009**, *131*, 18105–18111. (f) Breitenfeld, J.; Scopelliti, R.; Hu, X. *Organometallics* **2012**, *31*, 2128–2136.
- (23) (a) Kownacki, I.; Kubicki, M.; Marciniak, B. *Inorg. Chim. Acta* **2002**, *334*, 301–307. (b) Marshak, M. P.; Nocera, D. G. *Inorg. Chem.* **2013**, *52*, 1173–1175.
- (24) (a) Beckmann, J.; Jurkschat, K.; Schollmeyer, D. *Organosilicon Chemistry III: From Molecules to Materials*; Auner, N.; Weis, J., Eds.; Wiley: Weinheim, Germany, 1997; pp 403–406. (b) Fridrichová, A.; Mairychová, B.; Padělková, Z.; Lyčka, A.; Jurkschat, K.; Jambor, R.; Dostál, L. *Dalton Trans.* **2013**, *42*, 16403–16411.
- (25) Caulton, K. G. *New J. Chem.* **1994**, *18*, 25–41.
- (26) Tilley, T. D. *Acc. Chem. Res.* **1993**, *26*, 22–29.
- (27) Woo, H.-G.; Heyn, R. H.; Tilley, T. D. *J. Am. Chem. Soc.* **1992**, *114*, 5698–5107.
- (28) Sadow, A. D.; Tilley, T. D. *J. Am. Chem. Soc.* **2005**, *127*, 643–656.
- (29) The k_H/k_D value was obtained from integration of the ^{31}P NMR signals for complexes 1-H and 1-D generated from the room-temperature reaction of 1-OSiMe₃ with 1:1 Ph₂SiH₂/Ph₂SiD₂. The measurements were made when 1-OSiMe₃ was completely consumed, at which point we had observed no side reaction such as the formation of silyl derivatives. (See Supporting Information for details.)
- (30) Hartwig, J. F.; Bhandari, S.; Rablen, P. R. *J. Am. Chem. Soc.* **1994**, *116*, 1839–1844.
- (31) It should be noted, however, that our studies did not furnish any spectroscopic evidence supporting the involvement of Ni^{IV}(hydrido) silyl species; moreover, no Ni^{IV} species stabilized by bulky pincer ligands has been reported to date or even observed by spectroscopic techniques. Nevertheless, a stepwise reaction mechanism involving oxidative addition and reductive elimination cannot be ruled out for d⁸Ni^{II} because there is precedent for one well-defined silyl-based Ni^{IV} species bearing a neutral diphosphine ligand. (a) Shimada, S.; Rao, M. L. N.; Tanaka, M. *Organometallics* **1999**, *18*, 291–293. For other examples of convincingly characterized Ni^{IV} complexes, see (b) Klein, H.-F.; Bickelhaupt, A.; Jung, T.; Cordier, G. *Organometallics* **1994**, *13*, 2557–2559. (c) Klein, H.-F.; Bickelhaupt, A.; Lemke, M.; Sun, H.; Brand, A.; Jung, T.; Röhr, C.; Flörke, U.; Haupt, H.-J. *Organometallics* **1997**, *16*, 668–676. (d) Dimitrov, V.; Linden, A. *Angew. Chem., Int. Ed.* **2003**, *42*, 2631–2633. (e) Chen, W.; Shimada, S.; Tanaka, M.; Kobayashi, Y.; Saigo, K. *J. Am. Chem. Soc.* **2004**, *126*, 8072–8073. (f) Carnes, M.; Buccella, D.; Chen, J. Y.-C.; Ramirez, A. P.; Turro, N. J.; Nuckolls, C.; Steigerwald, M. *Angew. Chem., Int. Ed.* **2009**, *48*, 290–294. (g) Camasso, N. M.; Sanford, M. S. *Science* **2015**, *347*, 1218–1220. (h) Bour, J. R.; Camasso, N. M.; Sanford, M. S. *J. Am. Chem. Soc.* **2015**, *137*, 8034–8037.
- (32) A similar reactivity has been observed in the reaction of Cp′₂CeH with the silyl ether MeOSiMe₃(Cp′ = η⁵-1,2,4-t-Bu₃-C₅H₂): a σ-bond metathesis pathway breaks the O–Si and Ce–H bonds and forms new Ce–O and Si–H bonds, thus giving Cp′₂Ce(OMe) and Me₃SiH. See Werkema, E. L.; Yahia, A.; Maron, L.; Eisenstein, O.; Andersen, R. A. *Organometallics* **2010**, *29*, 5103–5110.
- (33) (a) Steigerwald, M. L.; Goddard, W. A., III. *J. Am. Chem. Soc.* **1984**, *106*, 308–311. (b) Thompson, M. E.; Baxter, S. M.; Bulls, A. R.; Burger, B. J.; Nolan, M. C.; Santarsiero, B. D.; Schaefer, W. P.; Bercaw, J. E. *J. Am. Chem. Soc.* **1987**, *109*, 203–219. (c) Rappé, A. K.; Upton, T. H. *J. Am. Chem. Soc.* **1992**, *114*, 7507–7517. (d) Balcells, D.; Clot, E.; Eisenstein, O. *Chem. Rev.* **2010**, *110*, 749–823.
- (34) (a) Brook, A. G.; Bassindale, A. R. In *Rearrangements in Ground and Excited States*; de Mayo, P., Ed.; Academic Press: New York, 1980; Vol. 2, pp 149–227. (b) Brook, A. G. *Acc. Chem. Res.* **1974**, *7*, 77–84. (c) West, R.; Lowe, R.; Stewart, H. F.; Wright, A. *J. Am. Chem. Soc.* **1971**, *93*, 282–283. (d) Wright, A.; West, R. *J. Am. Chem. Soc.* **1974**, *96*, 3222–3227. (e) Wright, A.; West, R. *J. Am. Chem. Soc.* **1974**, *96*, 3227–3232. (f) West, R. *Adv. Organomet. Chem.* **1977**, *16*, 1–31. (g) Reetz, M. T. *Adv. Organomet. Chem.* **1977**, *16*, 33–65.
- (35) Recall that concerted σ-bond metathesis reactions are very sensitive to steric bulk. Corey, J. Y. In *Advances in Silicon Chemistry*; Larson, G.L., Ed.; JAI: Greenwich, CT, 1991; Vol. 1, pp 327–387.
- (36) It is worth mentioning that the ^{31}P NMR spectrum of the reaction of 1-OSiMe₃ with excess Ph₂SiH₂ displayed a small peak at ca. 177.7 ppm during the initial phase of this reaction; this peak was gradually replaced by that of 1-H, indicating that the initially formed species (probably 1-OSiHPh₂) reacts further with Ph₂SiH₂ to give 1-H. It appears, therefore, that both pathways TSα and TSβ might also be operating in the reaction of 1-OSiMe₃ with Ph₂SiH₂ but not to the same extent as seen in the analogous reaction of Ph₃SiH.
- (37) For comparison, the ^{31}P resonances for the silyl species 1-SiPhH₂ appears at 200.7 ppm. It should be noted that in general the complexes 1-X give rise to ^{31}P signals that are 3–7 ppm downfield of the corresponding resonances for 2-X.
- (38) The closeness of the ^{31}P resonances for the species B under discussion and the triflate derivative (ca. 185 vs 184 ppm in C₆D₆)^{10c} suggests that species B might be the hydroxyl derivative which could be generated in situ via hydrolysis of a siloxide.
- (39) (a) Castonguay, A.; Sui-Seng, C.; Zargarian, D.; Beauchamp, A. L. *Organometallics* **2006**, *25*, 602–608. (b) Herbert, D. E.; Ozerov, O. V. *Organometallics* **2011**, *30*, 6641–6654.
- (40) For examples of such attacks on the phosphinite moiety in complexes (POC_{sp}³OP)NiX, see ref 11a.
- (41) It should be noted that the mixture of Ni(COD)₂ and POC_{sp}³HOP generated multiple species represented by several ^{31}P peaks at 155–157 and 167–168 ppm.
- (42) (a) Curtis, M. D.; Epstein, P. S. *Adv. Organomet. Chem.* **1981**, *19*, 213–225. (b) Ojima, I.; Inaba, S.; Kogure, T.; Nagai, Y. *J. Organomet. Chem.* **1973**, *55*, C7. (c) Pannell, K. H.; Brun, M. C.; Sharma, H.; Jones, K.; Sharma, S. *Organometallics* **1994**, *13*, 1075–1077. (d) Park, S.; Kim, B. G.; Göttker-Schnetmann, I.; Brookhart, M. *ACS Catal.* **2012**, *2*, 307–316.
- (43) (a) Straus, D. A.; Grumbine, S. D.; Tilley, T. D. *J. Am. Chem. Soc.* **1990**, *112*, 7801–7802. (b) Grumbine, S. D.; Tilley, T. D.; Rheingold, A. L. *J. Am. Chem. Soc.* **1993**, *115*, 358–360. (c) Grumbine, S. D.; Mitchell, G. P.; Straus, D. A.; Tilley, T. D.; Rheingold, A. L. *Organometallics* **1998**, *17*, 5607–5619. (d) Wanandi, P. W.; Glaser, P. B.; Tilley, T. D. *J. Am. Chem. Soc.* **2000**, *122*, 972–973.
- (44) (a) Tilley, T. D. *Transition-Metal Silyl Derivatives*. In *The chemistry of organic silicon compounds*; Patai, S., Rappoport, Z., Eds.; Wiley: New York, 1989; p 1415. (b) Tilley, T. D. In *The Silicon-Heteroatom Bond*; Patai, S., Rappoport, Z., Eds.; Wiley: New York, 1991; p 245. (c) Waterman, R.; Hayes, P. G.; Tilley, T. D. *Acc. Chem. Res.* **2007**, *40*, 712–719.

(45) (a) Mork, B. V.; Tilley, T. D. *Angew. Chem., Int. Ed.* **2003**, *42*, 357–360. (b) Mork, B. V.; Tilley, T. D.; Schultz, A. J.; Cowan, J. A. *J. Am. Chem. Soc.* **2004**, *126*, 10428–10440.

(46) (a) Mork, B. V.; Tilley, T. D. *J. Am. Chem. Soc.* **2001**, *123*, 9702–9703. (b) Mork, B. V.; Tilley, T. D. *J. Am. Chem. Soc.* **2004**, *126*, 4375–4385.

(47) (a) Glaser, P. B.; Tilley, T. D. *Organometallics* **2004**, *23*, 5799–5812. (b) Hayes, P. G.; Beddie, C.; Hall, M. B.; Waterman, R.; Tilley, T. D. *J. Am. Chem. Soc.* **2006**, *128*, 428–429.

(48) Mitchell, G. P.; Tilley, T. D. *Organometallics* **1998**, *17*, 2912–2916.

(49) (a) Feldman, J. D.; Peters, J. C.; Tilley, T. D. *Organometallics* **2002**, *21*, 4065–4075. (b) Peters, J. C.; Feldman, J. D.; Tilley, T. D. *J. Am. Chem. Soc.* **1999**, *121*, 9871–9872. (c) Calimano, E.; Tilley, T. D. *J. Am. Chem. Soc.* **2008**, *130*, 9226–9227.

(50) Mitchell, G. P.; Tilley, T. D. *Angew. Chem., Int. Ed.* **1998**, *37*, 2524–2526.

(51) A very recent report has described an analogous Si-to-Pt α -H migration taking place in a PSiP-type pincer complex. DeMott, J. C.; Gu, W.; McCulloch, B. J.; Herbert, D. E.; Goshert, M. D.; Walensky, J. R.; Zhou, J.; Ozerov, O. V. *Organometallics* **2015**, *34*, 3930–3933.

(52) For examples of Ni complexes bearing stabilized silylene ligands, see (a) Denk, M.; Hayashi, R. K.; West, R. *J. Chem. Soc., Chem. Commun.* **1994**, 33–34. (b) Gehrhus, B.; Hitchcock, P. B.; Lappert, M. F.; Maciejewski, H. *Organometallics* **1998**, *17*, 5599–5601. (c) Schmedake, T. A.; Haaf, M.; Paradise, B. J.; Powell, D. R.; West, R. *Organometallics* **2000**, *19*, 3263–3265. (d) Avent, A. G.; Gehrhus, B.; Hitchcock, P. B.; Lappert, M. F.; Maciejewski, H. *J. Organomet. Chem.* **2003**, *686*, 321–331. (e) Kong, L.; Zhang, J.; Song, H.; Cui, C. *Dalton Trans.* **2009**, 5444–5446. (f) Meltzer, A.; Inoue, S.; Präsang, C.; Driess, M. *J. Am. Chem. Soc.* **2010**, *132*, 3038–3046.

(53) Tanaka's group has reported a dimeric complex featuring a Ni₂Si₂ unit that is touted to consist of Ni^{III} nuclei bridged by silylene moieties originating from a 1,2-disilylbenzene, but ambiguities pertaining to the Ni–Ni and Si–Si interactions complicate the characterization of this compound as an authentic Ni-silylene: Shimada, S.; Rao, M. L. N.; Hayashi, T.; Tanaka, M. *Angew. Chem., Int. Ed.* **2001**, *40*, 213–216.

(54) Feldman, J. D.; Mitchell, G. P.; Nölte, J.-O.; Tilley, T. D. *J. Am. Chem. Soc.* **1998**, *120*, 11184–11185.

(55) Iluc, V.; Hillhouse, G. L. *J. Am. Chem. Soc.* **2010**, *132*, 11890–11892.

(56) It should be noted that some or all of the observed Si–Si bond forming reactions be promoted by Ni particles generated in situ from the decomposition of the pincer complexes. Indeed, Boudjouk et al. have reported that Ni particles generated in situ (by reduction) in the presence of phenylsilanes lead to Si–Si bond formations; however, the products of such reactions are invariably dimers, trimers, and tetramers only, never higher polysilanes. (See ref 6a above.) Moreover, even the action of Ni particles in this system appears to depend (at least partly) on the presence of solubilizing/stabilizing ligands, and it is crucial that the particles be generated in situ because metallic powder is inert.

(57) Vabre, B.; Lindeperg, F.; Zargarian, D. *Green Chem.* **2013**, *15*, 3188–3194.